Electronic Supplementary Information for

Engineering electronic structure of Two-Dimensional Subnanopore nanosheet by Molecular Titanium-oxide Incorporation for Enhanced photocatalytic activity

Table of contents

S1.Experimental Section

Preparation of 2D g-CN nanosheets

The 2D g-CN nanosheets were synthesized according to our previous reported literature.[1] In detail, 1 g of dicyanodiamide powder and 5 g ammonium chloride were dissolved in 30 ml water and frozen in liquid nitrogen. Then mixture was freeze-dried in a bulk tray dryer with the pressure of 0.035 mbar and a sublimating temperature of −50 °C for evaporating the water. Finally, the obtained white powder polymerized in a covered ceramic container at 550℃ for 4h at a rate of 3℃/min.

Preparation of 2D TiO-CN nanosheets

Firstly, 1 g of dicyanodiamide powder and 5 g ammonium chloride were dissolved in 27 ml, 23 ml or 15 ml water, noted as “solution A1, A2 or A3”. Then “solution A” was cooled with cool water for 3min. Secondly, 1 ml $TiCl_4$ liquid was added in 300 ml solution with 50 g ammonium chloride and stirred for 10 min to get a homogeneous solution, noted as “solution B”. After that, 3 ml, 7 ml or 15 ml “solution B” was added in the cooled “solution A1, A2 or A3”, respectively, getting colorless and transparent solution C. Finally, the “solution C” was also freeze-dried and the obtained white powder polymerized in a covered ceramic container at 550℃ for 4h at a rate of 3℃/min. The obtained TiO-CN samples were noted as TiO-CN1, TiO-CN2 and TiO-CN3 according to the amount of “solution A”.

Characterizations

X-ray powder diffraction (XRD) was carried out by using a Philips X’Pert Pro Super diffractometerwith Cu Kα radiation (λ = 1.54178 Å). X-ray photoelectron spectra (XPS) were performed on an ESCALAB MK II X-ray photoelectron spectrometer with Mg Kα as the excitation source. The transmission electron microscopy (TEM) was taken on a JEM-2100F field emission electron microscope at an acceleration voltage of 200 kV. The field emission scanning electron microscopy (FE-SEM) images were acquired on a JEOL JSM-6700F SEM. Atomic force microscopy (AFM) image was carried out on a DI Innova scanning probe microscope. The high-angle annular dark- field scanning transmission electron microscopy (HAADF-STEM) image and EDS mapping images were taken on a JEOL JEM-ARF200F atomic resolution analytical microscope. The Fourier transform infrared (FT-IR) experiment was taken on a Magna-IR750 FT-IR spectrometer in a KBr pellet. The photoluminescence (PL) spectrum was performed by FLUOROLOG-3-TAU fluorescence spectrometer equipped integrating sphere. The EIS and photocurrent were measured with three electrodes at 0.8 V (vs. Ag/AgCl) in 0.5 M Na_2SO_4 and Pt electrode were used as the counter electrode. XAS spectra at Ti K-edges were collected in the transmission mode with a Si (111) double-crystal monochromator at the BL14W1 station of the Shanghai Synchrotron Radiation Facility (SSRF). The SSRF ring storage operates at 3.5 GeV with a maximum current of 300 mA. XAS data have been analyzed by using the IFEFFIT package following standard procedures.

Photocatalytic test

•OH radical reactions were carried out as following: 5 mg of CN or TiO-CN was suspended in 80 mL aqueous solution, which contains 3 mM terephthalic acid and 0.01 M NaOH. Before exposure to light, the corresponding suspension was stirred in dark for about 25 min. During the light irradiation process, 5 mL of the solution was removed every 5 min and then centrifuged for the following measurement. The fluorescence signal of the 2-hydroxy terephthalic acid generated in the solution was gained on a fluorescence spectrophotometer with the excitation light wavelength of 320 nm.

ESR spectra were performed in the solution containing 1mg/ml sample (CN or TiO-CN samples) with the same amount of DMPO liquid. Before the ESR measurement, the solution was kept in the dark. The irradiation time was about 30 s.

Photodegradation of RhB was conducted as following: 50 mg of CN or TiO-CN was suspended in 100 mL of 2×10^{-5} mol/L RhB aqueous solution. The suspension was stirred in the dark for 30 min to get an adsorption-desorption equilibrium before light irradiation. During the degradation, 5 mL of the suspension was collected at a regular interval of 5 min. The suspension was concentrated and the solution was measured with a UV-3600 Shimadzu spectroscope. The concentration of RhB was estimated by monitoring the changes of absorption at 553 nm.

S2. XRD pattern, FT-IR spectra, SEM, TEM and HAADF-STEM images of 2D CN and TiO-CN nanosheets

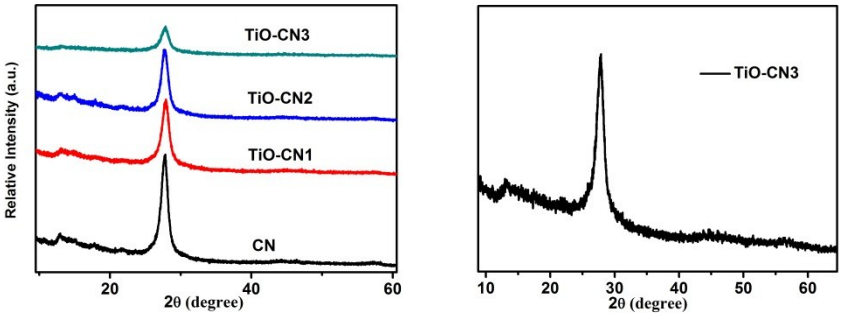

Figure S1. The XRD patterns of CN and TiO-CN samples.

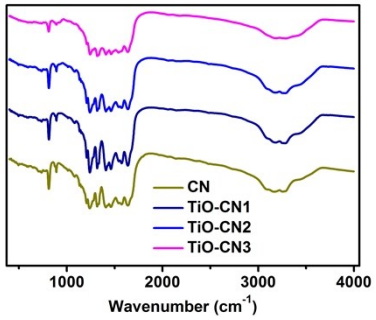

Figure S2. The IR spectra of CN and TiO-CN samples.

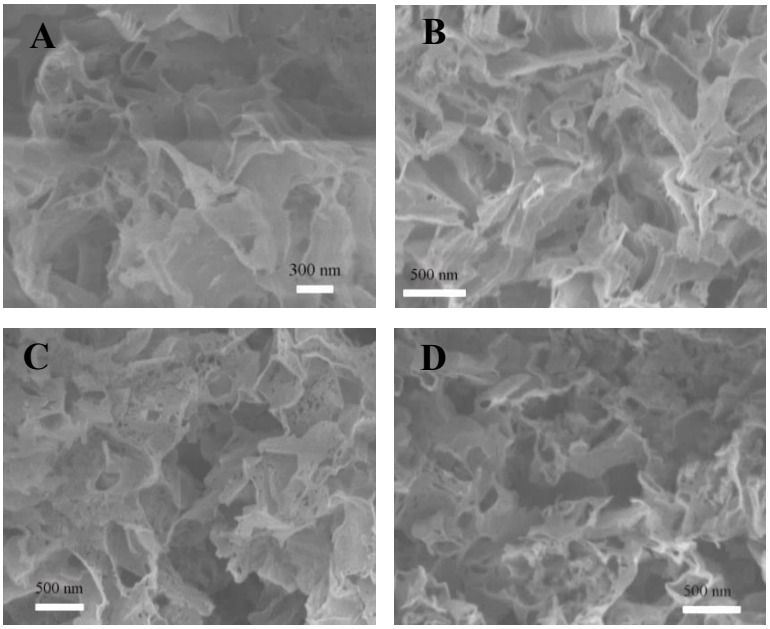

Figure S3. SEM images of CN (A), TiO-CN1 (B), TiO-CN2 (C), TiO-CN3 (D), respectively.

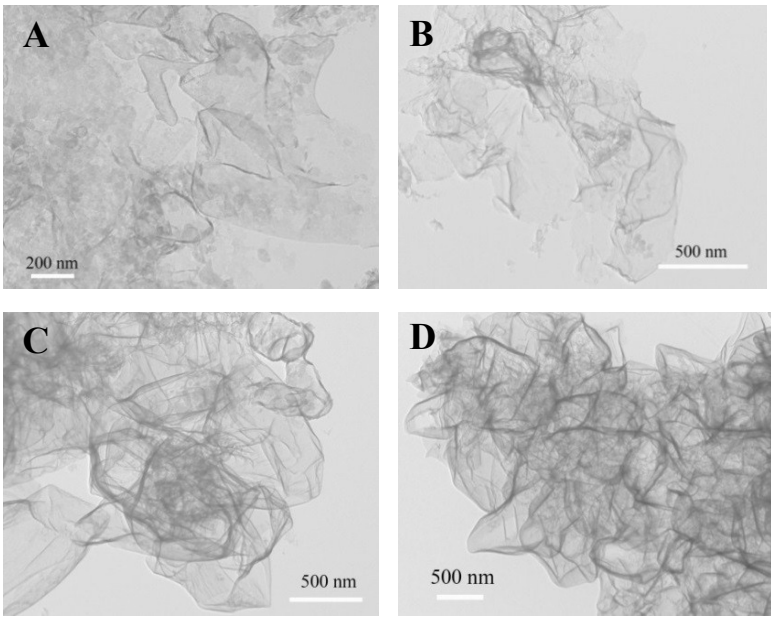

Figure S4. TEM images of CN (A), TiO-CN1 (B), TiO-CN2 (C), TiO-CN3 (D), respectively.

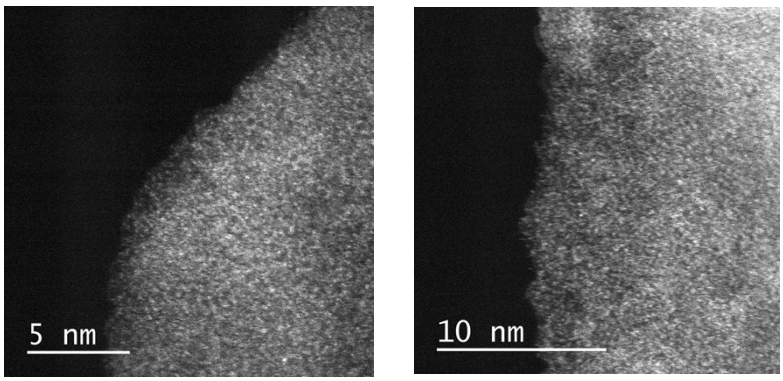

Figure S5.The HAADF-STEM images of TiO-CN2 nanosheets.

It should be noted that the C, N, O atoms were not visible in the HAADF-STEM image due to their low atomic weight. However, the contrast in the image enables the obvious identification of atomic scale of Ti in the CN matrix.

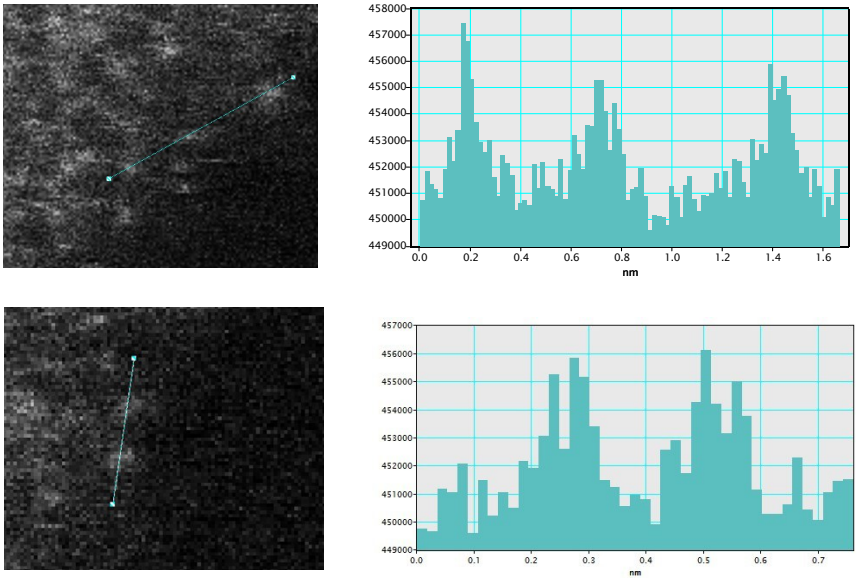

Figure S6. The enlarged HAADF-STEM image of TiO-CN (Left) and the intensity profile measured over the line marked in the left image (Right).

S3.The elemental mapping images of obtained TiO-CN2 nanosheet

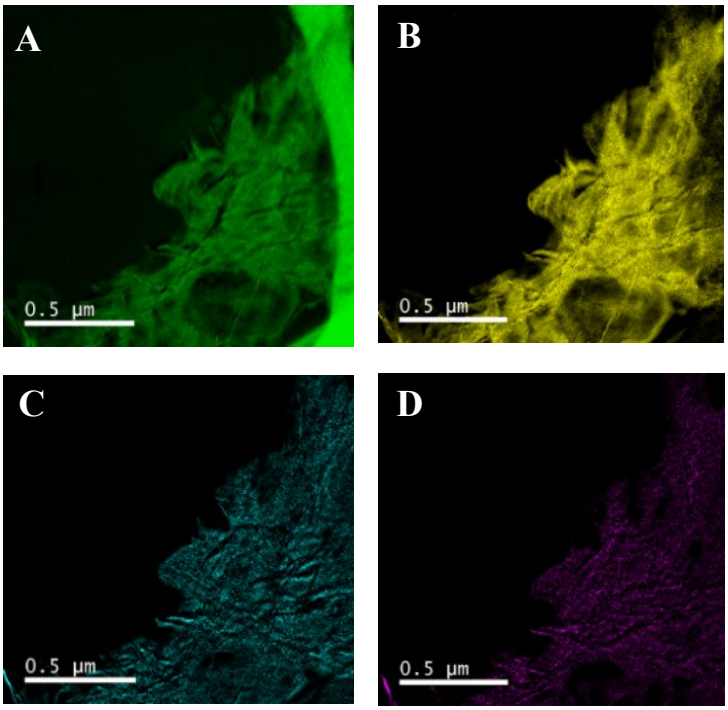

Figure S7. The corresponding EDS mapping images of titanium-oxide incorporated CN ultrathin nanosheet, indicating the homogeneous distribution of carbon (A), Nitrogen (B), Titanium (C) and oxygen (D).

S4. XPS and XAFS results of TiO-CN2 nanosheets

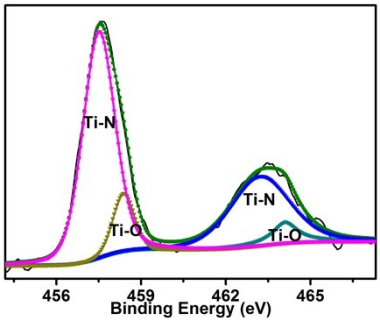

Figure S8. High resolution XPS spectra of Ti in TiO-CN2.

XPS was also used to understand chemical environment of the titanium-oxide in the 2D TiO-CN2 nanosheet. As shown in Figure S7, a typical spectrum of Ti reveals two kinds of chemically

bonding assigned to Ti-N (457.5 ev and 463.2 eV) and Ti-O (464.1 eV and 458.4 eV).[2,3] The ratio of Ti-O and Ti-N is about 1:6 according to the area ratio of Ti 2p peaks as shown in Table S1, giving chemical composition in form of $C_3N_4Ti_{0.1}O_{0.1}$. Combined with the XPS result of O in Figure S8, the chemical environment of Ti atom could be regard as one Ti atom coordinating by one O atom and six N atoms in the "nitrogen pots". When the molecular titanium-oxide was introduced into the subnanopore of CN, the peaks assigned to C and N atoms in triazine rings in the high-resolution C1s and N1s spectra take on a slight high binding energy shift (Figure S8).[3] Because after the molecular titanium-oxide incorporating into the "nitrogen pots", the electron cloud density of C and N atoms, especial the N atoms, would decrease and result into their high binding energy shift. In this regard, molecular titanium-oxide incorporation without destroying pristine matrix composition and structure holds promise for modulating electronic structure of 2D CN.

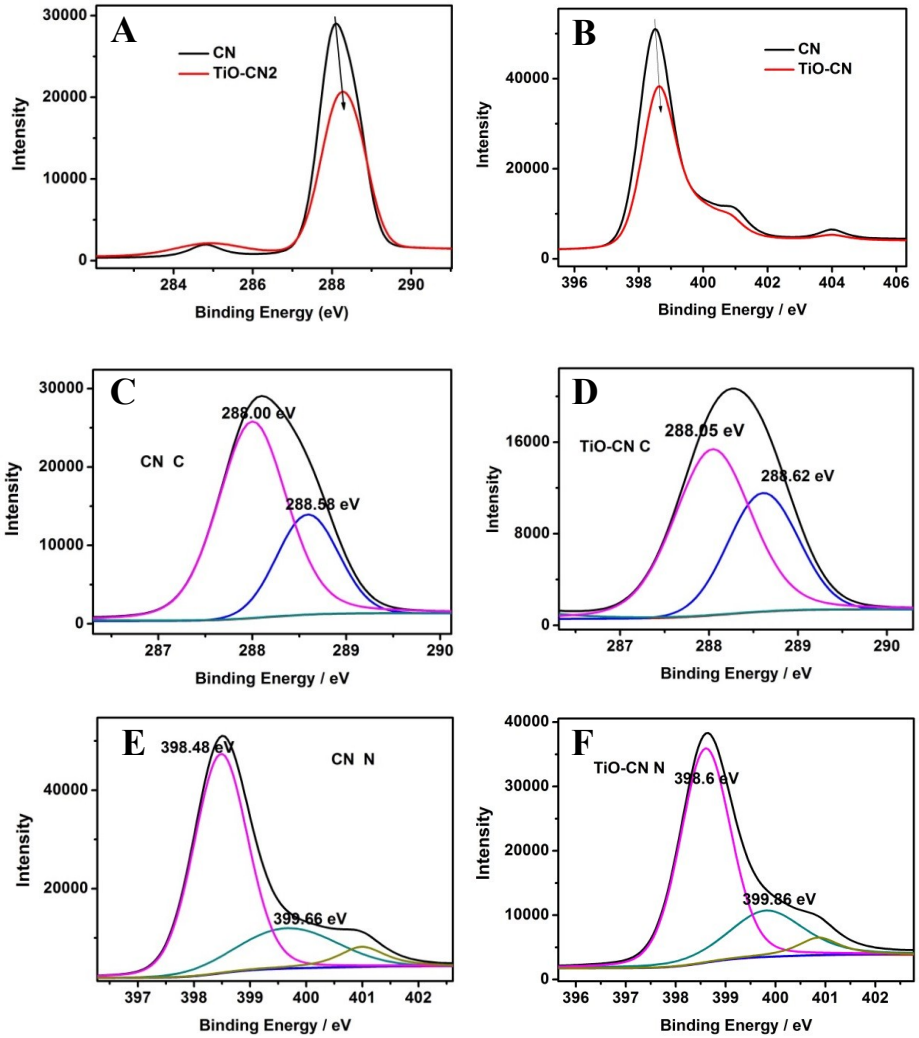

Figure S9. C 1s and N 1s XPS spectra of CN and TiO-CN2.

Figure S9A and B show the comparison of C1s and N1s XPS spectra of CN and TiO-CN2, respectively. The main peak in C1s spectra of CN (Figure S9C) can be deconvoluted into two peaks. The peaks located at 288.0 eV and 288.5 eV is attributed to sp^2-hybridized carbon in the N-containing aromatic structure. The two peaks in C1s spectra of TiO-CN2 (Figure S9D) shift to higher binding energy (288.0 eV and 288.6 eV) due to the introducing of Ti-O structure. The peak located at 398.4 eV and 399.6 eV in the N1s spectra of CN (Figure S9E) were commonly assigned to sp^2 hybridized nitrogen involved in triazine rings and bridging N atoms in tertiary nitrogen structure. And the two peaks in the N1s spectra (Figure S9F) also shift to higher binding energy (398.6 eV and 399.8eV) as the result of TiO structure incorporating in CN matrix.

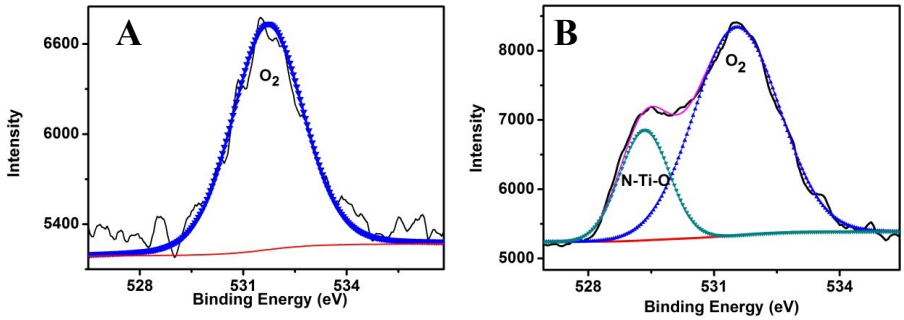

Figure S10. High-resolution XPS spectra of the O for 2D CN and TiO-CN2. The quantification of Ti 2p and O 1s peaks (at 529.34 eV) gives average Ti:O atomic ratio of nearly 1:1.

Table S1. The XPS results for TiO-CN2.

Element	At%	Peak area	Final ratio for TiO-CN2
C	**40.59**	**31752**	**3.0**
N	**52.78**	**68639**	**4.0**
Ti	**1.40**	**Ti-O**(433,724) **Ti-N**(2552,4329)	**0.1** (Ti-O:Ti-N=1:6)
O	**5.23**	**absorbed O_2**(7400) **O-Ti** (2590)	**0.1** (O-Ti)

The atoms ratios obtained from XPS were given in the Table S1. Through the analysis of the XPS results of TiO-CN2, the final ratios of element C, N, Ti and O were about $C_3N_4Ti_{0.1}O_{0.1}$

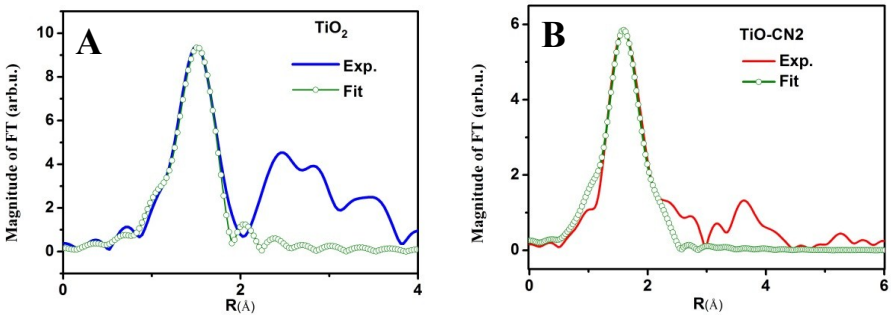

Figure S11. The quality of the EXAFS simulation for TiO_2 and TiO-CN2.

S5. The VB XPS and band gap results of TiO-CN2 nanosheets

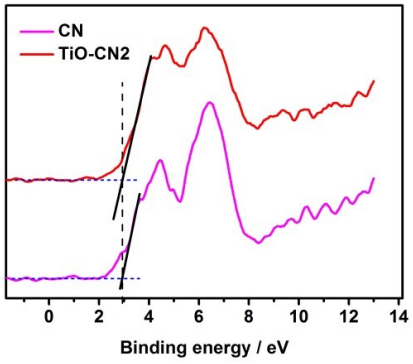

Figure S12. The VB XPS of CN and TiO-CN2.

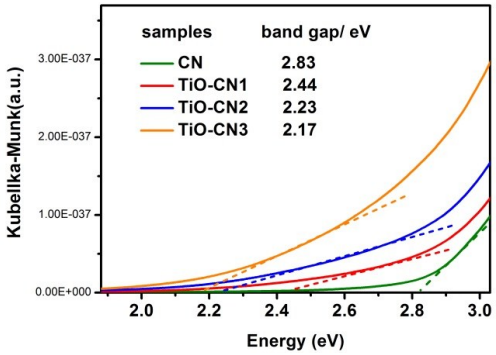

Figure S13. The plots of transformed Kubelka-Munk function vs photon energy for 2D CN and TiO-CN samples.

S6. Photocatalytic activity of CN and TiO-CN nanosheets

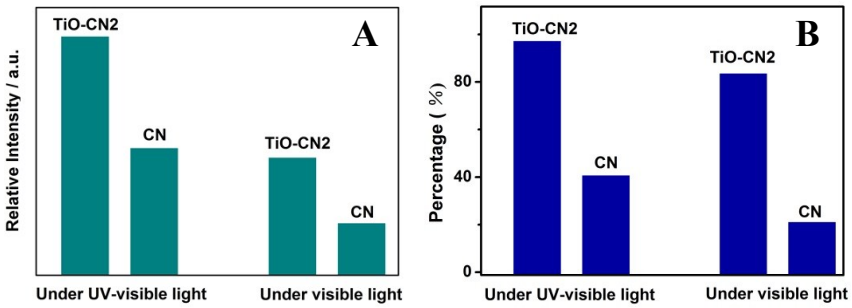

Figure S14. (A) Comparison of fluorescence signal intensity of 2-hydroxyterephthalic generated by reacting terephthalic acid with •OH radicals in the suspension of CN and TiO-CN2 samples under visible light (λ > 420 nm) and UV-visible light irradiation for 25 min. (B) Comparison of the percentage of degraded Rhodamine B by the CN and TiO-CN samples under visible light irradiation (λ > 420 nm) and UV-visible light irradiation for 5 min.

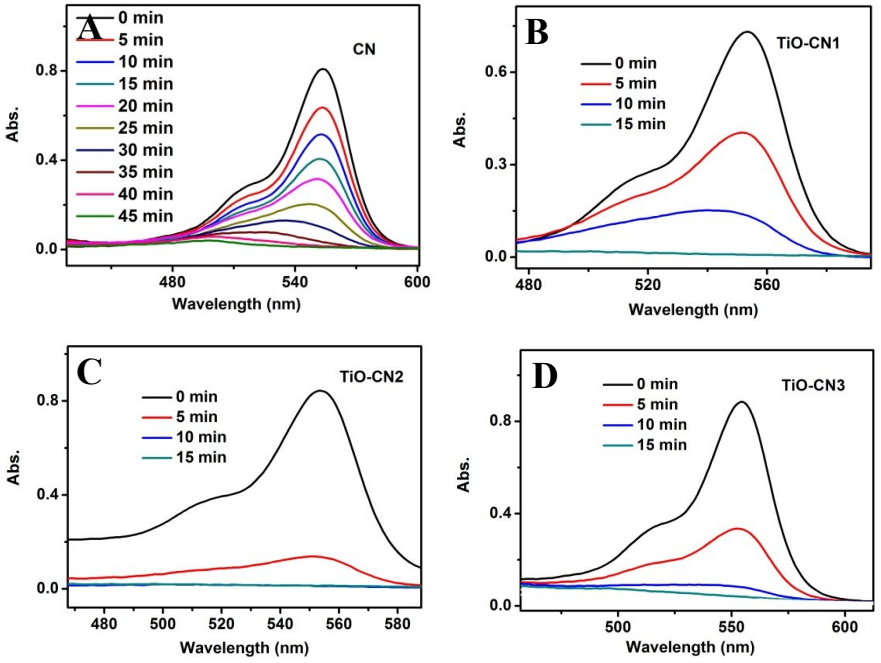

Figure S15. UV-visible absorption spectra changes of RhB aqueous solution after degradation by CN (A), TiO-CN1 (B), TiO-CN2 (C) and TiO-CN3 (D) under visible light.

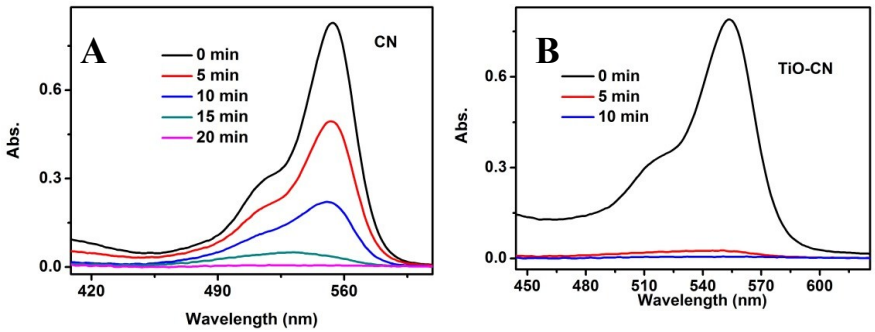

Figure S16. UV-visible absorption spectra changes of RhB aqueous solution after degradation by CN (A) and TiO-CN2 (B) under UV-visible light.

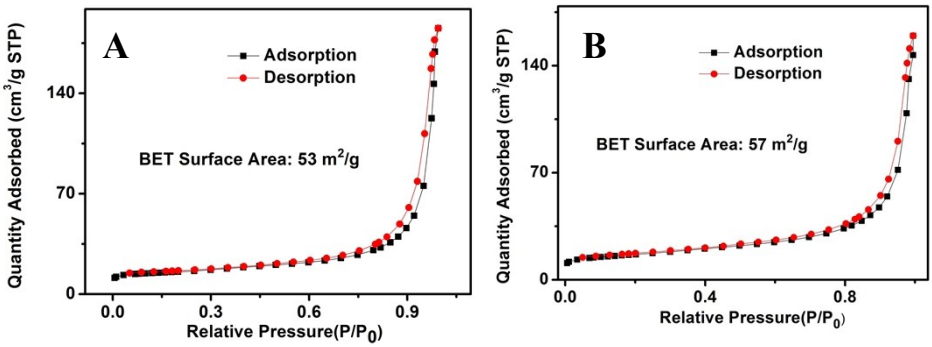

Figure S17. The N_2 adsorption-desorption isotherm of (A) CN and (B)TiO-CN2

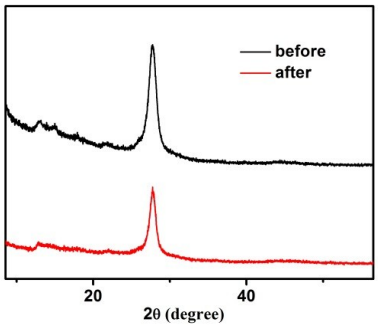

Figure S18. XRD patterns for TiO-CN2 before and after photocatalytic reaction.

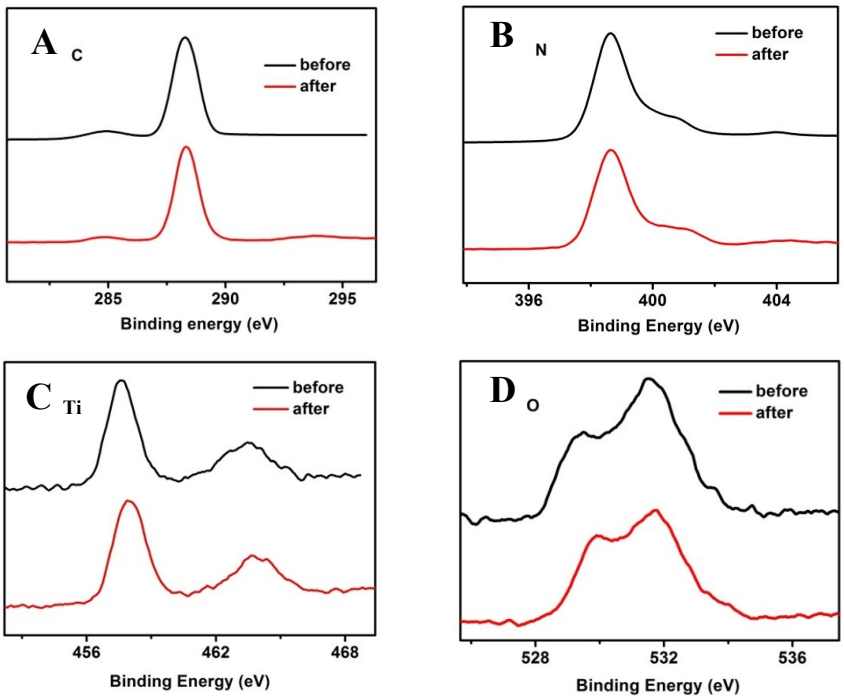

Figure S19. The high-resolution XPS spectra of the C (A), N (B), Ti (C) and O (D) for TiO-CN2 before and after photocatalytic reaction.

Reference:

[1] X. Lu, K. Xu, P. Chen, K. Jia, S. Liu, C. Wu, *J. Mater. Chem. A* **2014**, 2, 18924.

[2] T. Lin, C. Yang, Z. Wang, H. Yin, X. Lu, F. Huang, J. Lin, X. Xie, M. Jiang, *Energy Environ. Sci.* **2014**, 7, 967.

[3] M. Xing, F. Shen, B. Qiu, J. Zhang, *Sci. Rep.* **2014**, 4, 6341.

[4] P. Niu, L. Zhang, G. Liu, H.-M. Cheng, *Adv. Funct. Mater.* **2012**, 22, 4763.